Optics and Lasers in Engineering 151 (2022) 106875

Contents lists available at ScienceDirect

Optics and Lasers in Engineering

journal homepage: www.elsevier.com/locate/optlaseng

A single pixel tracking system for microfluidic device monitoring without image processing

Mingyang Ni, Huaxia Deng*, Xiaokang He, Yan Li, Xinglong Gong*

CAS Key Laboratory of Mechanical Behavior and Design of Materials, Department of Modern Mechanics, University of Science and Technology of China, Hefei, Anhui 230027, China

ARTICLE INFO

Keywords:
Image-free tracking
Single-pixel detection
Long-term
Real-time
Microfluidic device monitoring

ABSTRACT

Currently image-based optical measurement methods are the main approaches for detecting and tracking the movements of droplets or particles in microfluidic devices. However, the massive image data throughput and high computational consumption of image processing have become challenges to achieve real-time and long-term monitoring. Here a single-pixel tracking system is proposed to monitor the microfluidic device on the basis of single-pixel imaging and microscope technology without image reconstruction. The experimental results of tracking droplet in microfluidic device demonstrate that the proposed system have unique potential advantages in dynamic tracking for microfluidic devices. The data throughput of the proposed method is 1/792 of image-based methods and can reach an equivalent frame rate of 312.5 Hz with a low computational consumption of 89.3 μs per frame. The proposed image-free tracking method provides a welcomed boost to the further development of microfluidic device monitoring and indicates a potential way to real-time and long-term monitoring without image processing.

1. Introduction

Microfluidics devices, using channels from tens to hundreds of micrometers, are the systems that process or manipulate small amounts of fluidics (10^{-9} to 10^{-18} L) [1,2]. In order to monitor the working condition of microfluidics device, a lot of methods have been developed to measure the velocity field, pressure, flow rate, and particle trajectory [3,4]. Limited by the scale, traditional contact measurement, such as pressure gauge, fails to monitor microfluidics device for their potential impact on the flow field in microchannels. While image-based dynamic measurement approaches, based on image acquisition and processing, become the most popular sort because of non-contact measurement characteristics and rapid development of high-speed photography. However, the processing of massive amount of image data becomes challenge to achieve real-time and long-term monitoring for microfluidic device.

The earliest dynamic flow measurement is proposed in the Osborne Reynolds' pipe flow experiment [5], which utilized coloring agent to visualize the flow field and obtain the flow rate and manifold of the flow field by photography. With the advent of microscope, Reynolds' method was developed into an bright field observation method, by which movement of water head or colored fluid inside of microchannel can be observed and measured [6]. Latterly, Particle image velocimetry (PIV) method emerged as a whole-field, non-intrusive measurement technique where the fluid velocity is measured by recording the movement of tracer particles in the flow. Owing to the scale of the flow field in microchannels, it is impossible to use conventional PIV systems to obtain two orthogonal planes for optical access to the flow field. Subsequently, micro-PIV method [7,8] is developed by a volume illumination technique where the light source and the view field are induced through optic components. With this approach, the focal plane is moved down through the flow field to map the entire volume. The trace particles are assumed to have the same density as the surrounding fluid and neglectable influence for the flow. With help of high-speed camera, a modern commercial micro-PIV system can operate at high frame rate up to 10,000 Hz [9]. For different applications, micro-PIV with different light sources and scanning imaging systems have been developed, such as confocal laser scanning microscopy (CLSM) [4] and X-ray microimaging [10,11]. The spatial resolution can be improved accordingly but the frame rate becomes much lower, usually under 120 Hz, owing to the natively low efficiency of scanning imaging system. Molecular tagging velocimetry (MTV) [12] employs tag molecules instead of tracer particles and uses light of specific frequency to illuminate the tag molecules for imaging. MTV reduces the influence on flow field induced by tracer particles and is more suitable for biomedical microfluidic device observation.

However, all the systems mentioned above are based on image acquisition and image processing for dynamic analysis. When operating

* Corresponding authors.
E-mail addresses: hxdeng@ustc.edu.cn (H. Deng), gongxl@ustc.edu.cn (X. Gong).

https://doi.org/10.1016/j.optlaseng.2021.106875
Received 28 June 2021; Received in revised form 1 November 2021; Accepted 3 November 2021
0143-8166/

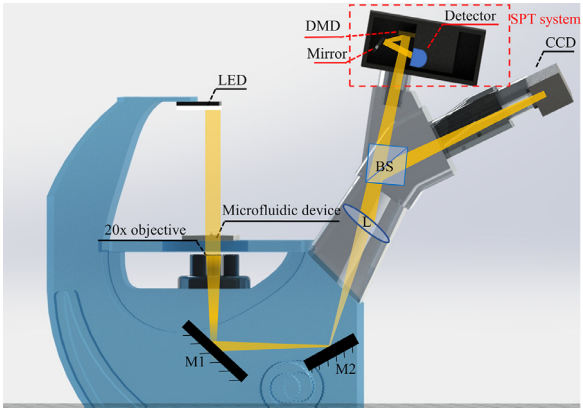

Fig. 1. Instrument configuration, M1 and M2 denote mirrors, L denotes lens and BS denotes beam splitter.

at high frame rate, the data throughput of image-based method is usually far more than the capability of data transport protocols. Thus, the images store temporally in Dynamic Random-Access Memory (DRAM) of high-speed camera before being transmitted to computer for subsequent processing. Owing to the insufficient memories of high-speed camera, short duration caused by high frame rate [13] limits application of image-based methods in long-term monitoring. Meanwhile, flow estimation and visualization are normally executed by cross-correlation-based algorithms [14,15] which require substantial computational resources to accurately estimate flow distributions. The computational consumption exceeds acquisition time, which makes real-time analysis not available. To meet the requirements of high-speed real-time and long-term monitoring task for microfluidic device, reducing the data throughput without decreasing the frame rate is the most possible approach.

This paper proposes another approach, an image-free method based on single-pixel imaging (SPI) theory [16–19], for monitoring microfluidic device. SPI is a method for reconstructing an image by processing the correlations between a series of predesigned illumination patterns and backscattered light intensity which is detected and transferred into electrical signal by a detector with no spatial resolution. More specifically speaking, SPI can directly extract the frequency domain coefficients, before the picture is reconstructed by implement of inverse Fourier transformation. By means of SPI [20–22], two specific coefficients from Fourier spectrum of the image can be extracted and utilized to get the path lines of single target object. A microfluidics device monitoring system is designed, constructed, and verified by experiments. The experimental results demonstrate that, for the proposed system, the computational consumption is less than data acquisition and the data throughput is 1/792 of traditional image-based methods, which indicates the potential of the proposed method to monitor the microfluidic device in a real-time, long-term and high frame rate way.

2. Experimental setup and data processing

The principle of the proposed system is that the movement of object in the scene shifts the phase distribution of Fourier domain without changing the amplitude distribution. The Fourier spectrum of interests is obtained by the single-pixel imaging theory to shrinks the data throughput and computational complexity. Details about system setup, methods of information extraction and other necessary processes are to be discussed in this section.

The instrument configuration, as shown in Fig. 1, includes illumination, spatially resolved optical system that provides visual magnification, single-pixel tracking (SPT) system, supplementary imaging system, data acquisition and processing system (omitted in the figure).

The SPT system consists of spatial light modulator (SLM), optic component and detector, which is constructed for obtaining certain Fourier spectrum of interests without imaging. A 12-watt plane LED serves as the illumination source, and transmitted light from the focal plane is collected and imaged on the surface of SLM where the spatial light modulation takes place.

Spatial light modulation is to program amplitude, phase of light waves in space and time. Digital micromirror device (DMD, Taxes Instruments DLP Discovery 4100 development kit) serves as the SLM in this system to conduct high-speed spatial light modulation. The DMD owns 1024 × 768 pitched programmable micro mirrors within plane of 0.7 inch and binary amplitude modulation is conducted by turning the micromirrors to different on and off states. Intensity of modulated light field is detected by a photomultiplier diode (Thorlabs, PMM02). The response of photomultiplier diode is converted into analog electric signals by a DAQ (Art Control, USB-3133A) operating at maximum sampling rate of 0.5 MHz. The signals are processed on the computer (Intel 7500, 3.4 GHz CPU,16GB RAM, 500GB SSD) to obtain the track of the moving object. In addition, a CCD (Hikvision, MV-CE060–10UM) works as the supplementary imaging system to compare tracking results of SPT techniques with traditional image-based methods.

An accustomed microfluidic device based on flow focusing is placed at the focal plane of the microscope (Sunny Optical, ICX40). The cross section of rectangular microchannel is 54 × 265 μm in size measured by digital microscope (KEYENCE VHX VH-Z100). The continuous phase is mineral oil. The dispersed phase is black ink dyed deionized water with a viscosity of 1.005 mPa•s in 20 °C, and their interfacial surface tension is 52 mN/m. The flow rates of two phases are manipulated by two high accurate syringe pumps (LSP02–1B, Longer Pump), respectively. Droplet of ink-dyed water is generated continuously by the microfluidic device as shown in Fig. 4(a), and experiments are carried out to measure the velocity of the moving droplet inside of microchannel. With a 20 × objective lens, these characteristics afford a dynamic measurement for flow rate ranged from 100 to 10,000 μm, which covers the working condition of common microfluidic device.

The schematic procedure of measuring chain of the proposed system is presented in Fig. 2 to obtain the velocity and trajectory of the moving target eventually. With the system mentioned above, the intensity of modulated light is turned into analog voltage signal, and the signals is stored on computer. 4-step phase shifting method is then employed to extract Fourier coefficients from the signals. Details about principle of Fourier basis modulation can be found in Supplementary Material S1. Given whole coefficients of Fourier spectrum, the real image can be obtained by implementation of inverse discrete Fourier transformation. However, for the system proposed in this paper, only two independent Fourier coefficients are needed, which is the key to reduce the data throughput.

For every frame, 8 Fourier basis patterns are generated, binarized and displayed on the DMD to get two Fourier coefficients. The patterns are 1024 × 768 pixels in size to cover the surface of DMD. The former 4 patterns shown in Fig. 3(a–d) share a spatial frequency pair (f_x = 0, f_y = 2/768) and only differ in initial phase φ. They are utilized to extract C(0, f_y), which denotes one specific coefficient in Fourier spectrum with spatial frequency pair (0, f_y). Similarly, the later 4 patterns shown in Fig. 3(e–h) with spatial frequency pair (f_x = 2/1024, f_y = 0) are prepared for extraction of C(f_x, 0). The structured patterns are repeatedly displayed on the DMD in sequence. Note that Fig. 3(i) is the partial enlarged drawing of Fig. 3(d), indicating that the patterns are all binary rather than grayscales as they intuitively look like.

The basic working principle of the SPT system is that, any change in spatial domain affect the whole Fourier domain [16]. The displacement (x_0, y_0) of target object in spatial domain eventually results in phase shift ($-2\pi f_x x_0$, $-2\pi f_y y_0$) in Fourier domain, which can be expressed as:

$$I(x - x_0, y - y_0) = F^{-1}\{C(f_x, f_y) \cdot \exp[-j2\pi(f_x x_0 + f_y y_0)]\}, \quad (1)$$

Where F^{-1} denotes inverse Fourier transform operation. To track a specific moving object rather than the movement of scene, background

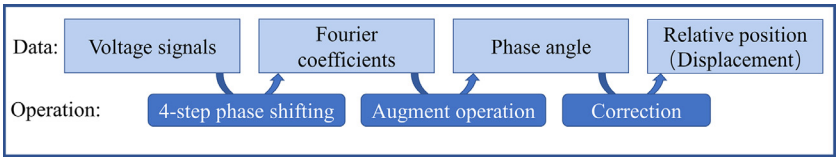

Fig. 2. Schematic of measuring chain.

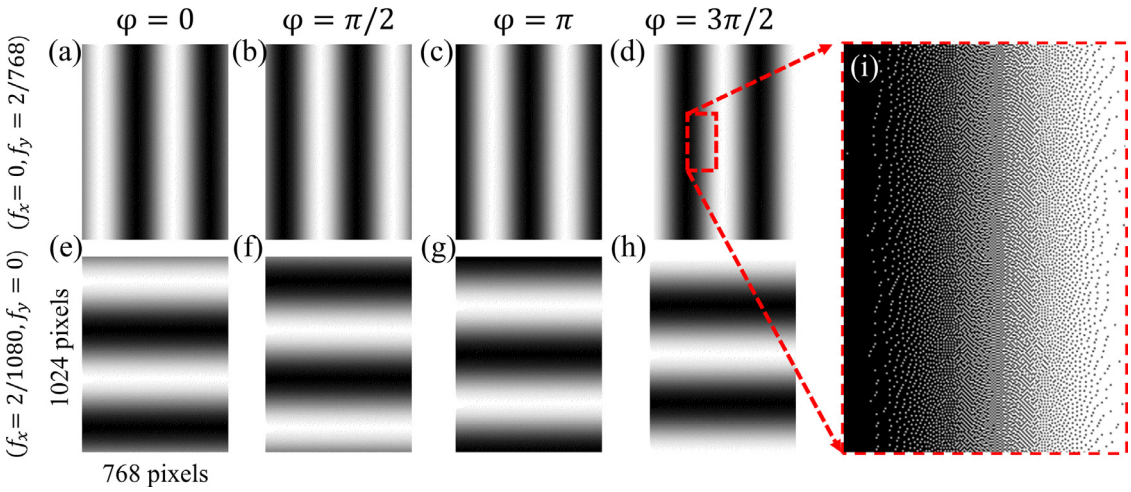

Fig. 3. Patterns for single-pixel tracking, (a-d) patterns for C(0, f_y); (e-h) patterns for C(fx, 0); (i) the partial enlarged drawing.

subtraction operation must be conducted by C(fx, f_y)- C_{bg}(fx, f_y). Here C_{bg}(fx f_y) refers to the Fourier coefficients obtained by patterns of frequency pair (fx, f_y) at the point when the object is out of scene or being static in the scene. In order to solve the equation, any two variable Fourier coefficients in x and y coordinates during the moving of an object can be utilized to form the equations' group. For simplicity, C(fx, 0) and C(0, f_y) have been chosen for the proposed system. After background subtraction, the displacement in two direction can be directly derived through:

$$x_0 = -\mathrm{Arg}\{C(fx, 0) - C_{bg}(fx, 0)\}/2\pi fx, \tag{2}$$

$$y_0 = -\mathrm{Arg}\{C(0, fy) - C_{bg}(0, fy)\}/2\pi fy, \tag{3}$$

Where the Arg{•} denotes argument operation. Eqs. (2) and (3) denote that only relative movement between the initial and current position can be figured out, while the exact position of the object is unknown. Meanwhile the background must be stationary in the whole operation. With the relative displacement of target object at every moment, the velocity and acceleration can be easily deduced through time difference.

Before experiments, both CCD and the SPT system demand initial pre-test calibration to determine those parameters necessary for conversion from pixels to real coordinates. A 0.01 mm stage micrometer depicted in Fig. 4(b) serves as the standard gauge. In terms of SPT system, the picture shown in Fig. 4(c) is obtained by Single-pixel imaging (SPI) [14]. The chosen spatial resolution is 128 × 128 pixels, which is low owing to the nature of SPI. For CCD, the gauge is set in the focal plane. Aperture and exposure time of CCD are adjusted to image the gauge clearly. The result by CCD is shown in Fig. 4(d). The calibration values, that indicates the ratio between the pixel value and the actual distance, are obtained by photogrammetric calibration principle [23] for both CCD and SPT system.

Another demonstration experiment that verifies the individual SPT system is recorded in Supplementary Material S2, showing the data processing procedure in details and the capability of tracing complex trajectories.

3. Theoretical verification

Theoretical verification is conducted here to reveal relationship between the selected frequency of patterns and phase changes. The stationary scene is 256 × 256 pixels in size and made of 4 white letters and grayscale background. The object (white block, 10 × 10 pixels) moves straightly in x direction with the speed of 1 pixel/s. Four groups of patterns with different fx but same f_y are used to obtain phase change in x direction, following the measuring chains mentioned above.

The results in Fig. 5(a) show that, for the same displacement, the phase angle multiplies with the spatial frequency. Due to the periodicity of the Fourier basis patterns, phase change will exceed 2π if the displacement within one frame interval is larger than a fringe period. In order to avoid unnecessary confusion, here a suggestion for choosing patterns of proper frequency is offered:

$$fx > 2V_{max(x)}/C_V N_x^2, \tag{4}$$

Where fx denotes the choosing frequency in x direction, $V_{max(x)}$ denotes the maximum of actual velocity of object in x direction, C_V denotes the calibration value and there are N_x pixels per row in the patterns. The rule works for selecting f_y as well.

Meanwhile, the result of argument operation is periodic and phase ambiguity occurs for programing where the values of measured phase angles step over $\pm\pi$. Therefore, phase angle correction must be conducted.

The phase angle curve is judged to have crossed a period when the adjacent two measured phase angles are with opposite sign and the absolute difference of them is larger than π. To obtain real difference between every two adjacent phase angles, either 2π or -2π is added to the measured difference accordingly. The corrected phase angles can be obtained through real differences and zero point assumption of the first measured phase angle. Take the simulation results of fx = 8/256 for instance, the measured phase angle is depicted in Fig. 5(b) with black line, and the corrected phase angle based on the rules mentioned above is presented as black dot line. Taking the very first corrected phase angle as zero, the displacement can be obtained through Eq. (2) as the blue line shown in Fig. 5(b). Note that this rule meets difficulties when the object moves so fast that the real phase angle flips over more than one

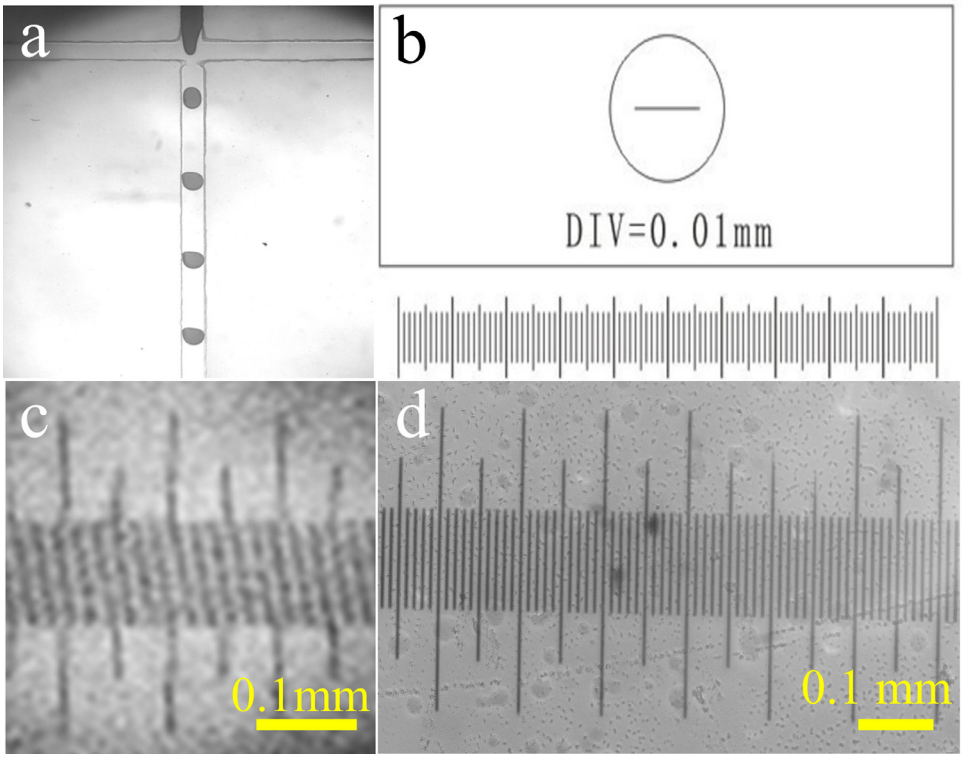

Fig. 4. (a) the microfluidic device observed by microscope;(b) the stage micrometer used for calibration;(c) the calibration picture for SPT system under 20 × objective lens, the spatial resolution is 128 × 128 pixels; (d) the calibration picture for CCD under 20 × objective lens, the spatial resolution is 3072 × 2048 pixels.

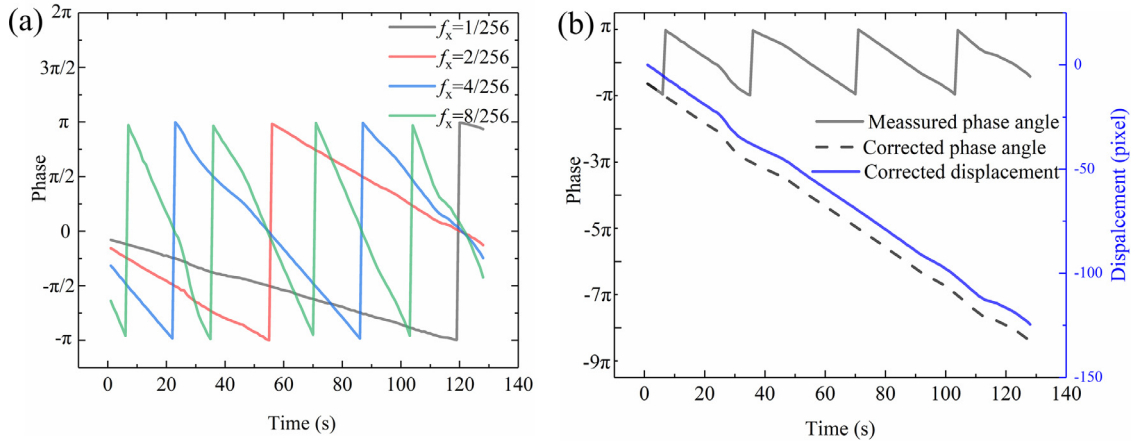

Fig. 5. (a) phase change about the same movement, using different Fourier frequency; (b) phase angle correction procedure for fx = 8/256.

period within interval of one frame. Thus, before experiments start, both the frame rate and the frequency of patterns must be adjusted according to the velocity of moving object.

4. Experiemntal results and discussion

Microfluidic device under different working conditions are monitored by both CCD and SPT system. The flow rate of dispersed phase is fixed at 10 μL/hour and flow rate of continuous phase varies from 20 to 180 μL/hour with an interval of 20 μL/hour. For simplicity, the flow rate ratio between continuous phase and dispersed phase is defined as the flow rate ratio K in this paper. With different K, dispersed droplets with different sizes and velocity are generated.

In the chosen field of view, the droplets are moving with a constant speed along the straight microchannel, where the velocity of droplet is the parameter of most interested. The average droplet velocity for different K is shown in Fig. 6 to compare the results of CCD and SPT system. The standard deviation of SPT system is less than 3%, and the average difference between SPT system and CCD is less than 10%. The largest difference occurs when flow rate ratio is 2. The measurement error is induced because of the large and slow droplet which is unable to totally leave the field of view before next droplet enters at this flow rate. Note that for $K > 4$, the average difference between SPT system and CCD is less than 5%.

To further verify the reliability of the results, the Bretherton relationship [24] is employed. Bretherton relationship denotes that, for droplets with approximate or larger than the microchannel cross section, there are lubrication films made of continuous phase between walls of microchannel and droplets where the capillary number (Cad) lower than 0.01. The existence of the film results in a difference between velocity of droplet and the external flow that transports the droplet. For droplet with smaller size than cross section of microchannels, the velocity of droplet is closed to flow rate.

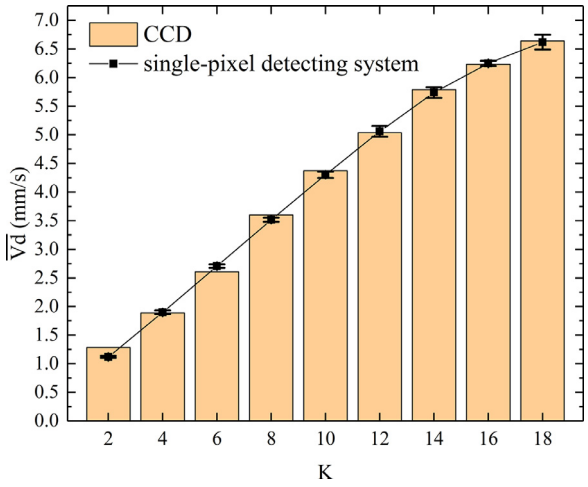

Fig. 6. Results of microscale experiments: variation in averaged droplet velocity $\overline{V_d}$ with flow rate ratio K, obtained by CCD and SPT system.

Table 1
Comparison between SPT system and original Single-pixel imaging.

	Spatial resolution(pixels)	measurement times	Maximum frame rate
SPT	786,432	2S(S = 2,3,4)	11,000/S Hz
SPI	N	2N	11,000/N Hz

For a rectangular microchannel, the velocity of droplet V_d is slower than the velocity of external flow V_{ex} and the Bretherton relationship satisfied is as followed.

$$(V_d - V_{ex})/V_d \propto -Ca_d^{-1/3}. \tag{5}$$

Here V_d is measured by tracking system, V_{ex} is calculated by 2-D Poiseuille law for rectangular channel [25], and Ca_d is the Capillary number of droplet can be obtained by:

$$Ca_d = \mu V_d/\sigma, \tag{6}$$

where μ is the viscosity of dispersed phase and σ is the interfacial tension between two phases.

The average length of the long and short axes of the elliptical droplet $\bar{D}$ is taken as the criteria to determine whether the size of droplet is large enough to meet Bretherton relationship. As the pictures taken by CCD shown in Fig. 7(a), the equivalent diameter $\bar{D}$ decreases with rise of flow rate ratio K. For $K > 10$, the droplet is contactless with walls visually. And for $K \leq 10$ the droplet is large enough to meet the Bretherton relationship, the boundary of two flow states is marked by a blue dot line in Fig. 7(a).

$$W = \left(V_{ex}/V_d - 1\right) \cdot Ca_d^{1/3} \tag{7}$$

is utilized to verify Bretherton relationship. As shown in Fig. 7(b), $Ca_d < 0.01$ is met for all flow rate ratio K in this experiment and W remains constant with $K \leq 10$, where the droplets are large enough and the lubrication films exist. With further increasement of K, the droplet become contactless with the walls of microchannel, and the W deviated from the Bretherton value starts to increase at this situation.

After verification, the proposed system is compared with high-frame-rate imaged-based method and original single-pixel imaging method considering resolution, speed and monitoring time. The comparison results of the former one is listed in Table 1.

The highest refreshing rate of DMD is 22,000 Hz under binary mode and the spatial resolution is 1024 × 768 pixels. In order to recover a N-pixel picture for obtaining the position of the object, the original Single-pixel imaging method has to measure the light intensity for 2 N times, which strictly limits real-time tracking within extremely low spatial resolution. In terms of SPT system, employing the S-step phase shift method (S = 2,3,4), the measurement times is always 2S for every frame. Differently from SPI method, SPT is not concerned about how many pixels are there in the field of view, and thus potential maximum frame rate of the proposed system is 5500 Hz (=22,000/4, S = 2).

For an optical system, the minimum resolvable distance d is

$$d \approx \frac{0.61}{f_c}, \tag{8}$$

where f_c is the cut-off frequency of the system. In optical system without considering the resolution of imaging system, the cut-off frequency is theoretically determined by the Numeric Aperture (NA) of lens and the wavelength λ. The minimum resolvable distance then is known as diffraction limit in optical system.

In SPT system, the frequency spectrum is designed by the structured pattern, which is directly related to the spatial resolution R_s and pattern design. The cut-off frequency thus can be expressed as

$$f_c \propto O(R_s), \tag{9}$$

Currently, the cut-off frequency of single pixel imaging system is far lower than the optical systems with CCDs. Thus, the spatial resolution of the proposed method for now is still far lower than the ones with CCDs. This cut-off frequency would rise with the development of higher spatial resolution SLM. Even higher resolution may achieve if combined with psychography technology [26] which has the ability to increase the cut-off frequency to break diffraction limit. Therefore, the proposed system offered a potential super-high-resolution tracking without increasing the accusation time theoretically. What's more, the proposed SPT system can achieve much higher resolution than SPI system since only spectrum of interests are needed for SPT systems. In order to discuss the monitoring duration of the proposed SPT system, the data throughput and other features of the proposed method are compared with HRI in actual experiments, which are listed in Table 2.

Firstly, the data throughput and duration for both methods are compared. The detector used is PDA100A2(Thorlabs), of which the bandwidth is 3000 Hz at 70 dB setting. Using 4-step phase shifting method, the upper limit is 3000/8 = 375 Hz. With the constraint of the response time (100 ns) of detector, 312.5 Hz is thus selected as the frame rate according to the previous proposed criteria. For every modulation pattern, 100 samples are averaged into one for calculation. Using 16-bit DAQ, the data throughput is 0.48 Mbps (= 16 bits (2 bytes) × 100 sample/frame × 2500 frame/s). For a normal high-speed camera operating at same frame rate and spatial resolution, the data throughput is 380.25 megabytes per second (= 1.17 Mbps × 312.5 fps), which is 792 times more than the proposed system. The data throughput of image-based method is evaluated by the data size of 1024 × 768 pixels. TIF-format photograph is captured by high-speed camera (Phantom, V2515). Apparently, the proposed system can operate in much longer duration than imaged based system. The monitoring duration is estimated by dividing 1 Terabytes storage with the data throughput per second for both SPT and high-speed camera at the same operative frame rate of 312.5 Hz. The results for both methods are listed in Table 2, which represents remarkable influence of shrinking data throughput on prolonging duration. Note that using better detector of higher bandwidth and lower response time, taking the PMT1001/M (Thorlabs) as an example, the maximum sampling rate referred in Table 2 can be easily achieved. Furthermore, by using phase shifting methods with less steps, such as 3-steps Fourier SPI [16] and 2-steps Fourier SPI [27], the maximum frame rate of the proposed system can be further increased. Therefore, the potential highest tracking frame rate for the proposed SPT system is 5500 Hz (= 22,000 refreshing rate/4 patterns per frame, using 2-steps phase shifting method).

Moreover, the real-time operation capabilities of both methods are compared. For SPT system, the average computational consumption of processing for one frame is 89.3 μs by a computer with an Intel 7500, 3.4 GHz CPU, 16GB RAM and MATLAB 2021a, which is far less than acquisition time of 3.2 ms and indicates that a real-time tracking is available with FPGA programming. However, computational consumption

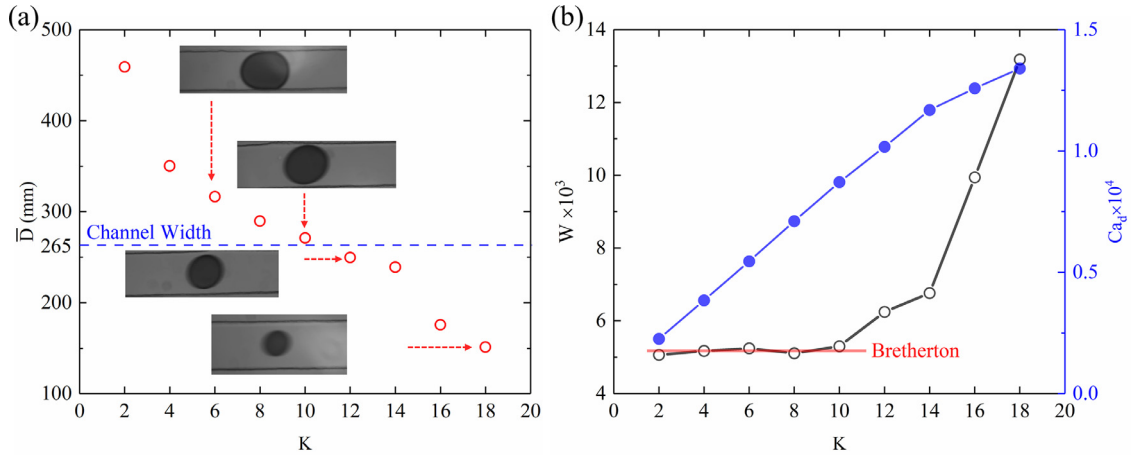

Fig. 7. Verification of Bretherton relationship: (a) variation in equivalent diameter of droplets with K, obtained by CCD;(b) Variation in W (black hollow circle) and Ca_d (blue solid circle) with flow rate ratio K, the red line represents Bretherton value.

Table 2
Comparison between SPT system and HRI system.

	Data throughput	Duration	Computational time	Acquisition time	Maximum frame rate
SPT	0.48 Mbps	25.8 days	89.3 μs	3.2 ms	5500 Hz
HRI	>300 Mbps	46 mins	>10 ms	<3.2 ms	>100,000 Hz

for HFRI system is more than acquisition time working with the same tracking frame rate. This comparison shows the merits of SPT system in less complexity of computation and its real-time operation capability.

It should be noted that the proposed monitoring system has three limitations. Firstly, different with image-based method, only one object moving in a stationary 2-D background can be tracked accurately and any deformation of the channels may result in inaccuracy of tracking. Secondly, the displacement obtained in this paper is a relative value and the exact position can only be obtained after calibration for the initial start point. The exact position of the tracking target in real-world coordinate is available on specific conditions when the object enters the field of view from upside or downside and leaves at left or right side, or under the exact opposite condition. But luckily, for the microfluidics monitoring task, the movement track of droplet is previously decided by the designed structure, which means the relative position is enough to obtain exact position of droplet. Lastly, the maximum spatial resolution for DMD is 1024×768, which is pretty low compared with commercial CCD. However, it is bound to be solved by spatial light modulator of higher spatial resolution.

The results and discussions show that the proposed SPT system is a reliable high-speed real-time and long-term way for microfluidic device monitoring. With this system, the real-time position of target object can be obtained. The velocity and acceleration can thus be obtained by temporal difference method. Therefore, other relative dynamic mechanics measurements such as pressure drop at exit is possible to be obtained on the basis of fluid mechanics. For example, using Poiseuille equation for different shapes of cross-section, the pressure difference can be obtained through the measured velocity. Overall, the proposed SPT system for microfluidic devices has the potential to monitor the velocity and other parameters in real time and last long duration.

5. Conclusion

In this paper, a single-pixel tracking system is proposed to achieve real-time, and long-term microfluidic process monitoring. By means of spatial light modulation, Fourier basis patterns are employed to get two values in Fourier domain of interests without imaging. Displacement of moving target object in stationary background can be obtained by phase shifting calculation. Experimental results demonstrate the proposed system can detect the trajectory and obtain the velocity of target object accurately. Working at frame-rate of 312.5 Hz, the data throughput of proposed system is only 1/792 of conventional high-speed-camera- based method. This work generates a different insight for the application of single-pixel imaging technology in an image-free way. For droplet or particle moving inside of microfluidic device, relative displacement can be obtained by the proposed system with far less data throughput and computational consumption compared with image-based system, which indicates a potential high-frame rate, real-time, and long-term approach to monitoring the microfluidic devices.

Funding

Financial supports from the National Natural Science Foundation of China (Grant No. 12132016), Strategic Priority Research Program of the Chinese Academy of Sciences (Grant No. XDB22040502) are gratefully acknowledged.

Declaration of Competing Interest

The authors declare that they have no known competing financial interests or personal relationships that could have appeared to influence the work reported in this paper.

Supplementary materials

Supplementary material associated with this article can be found, in the online version, at doi:10.1016/j.optlaseng.2021.106875.

CRediT authorship contribution statement

Mingyang Ni: Conceptualization, Methodology, Software, Writing – review & editing, Validation, Formal analysis. **Huaxia Deng:** Conceptualization, Methodology, Writing – review & editing, Supervision, Project administration. **Xiaokang He:** Methodology, Resources. **Yan Li:** Methodology, Resources. **Xinglong Gong:** Writing – review & editing, Supervision, Project administration, Funding acquisition.

References

[1] Gravesen P, Branebjerg J, Jensen OS. Microfluidics-a review. J Micromech Microeng 1993;3:168–82.
[2] Teh SY, Lin R, Hung LH, Lee AP. Droplet microfluidics. Lab Chip 2008;8:198–220.
[3] Van der Kindere J, Laskari A, Ganapathisubramani B, De Kat R. Pressure from 2D snapshot PIV. Exp Fluids 2019;60:32.
[4] Park JS, Kihm KD. Use of confocal laser scanning microscopy (CLSM) for depth-wise resolved microscale-particle image velocimetry (μ-PIV). Opt Lasers Eng 2006;44:208–23.
[5] Eckhardt B, Schneider TM, Hof B, Westerweel J. Turbulence transition in pipe flow. Annu Rev Fluid Mech 2007;39:447–68.
[6] Pan C, Chuang H, Cheng C, Yang C. Micro-flow measurement with a laser diode micro-particle image velocimetry. Sens Actuators A Phys 2004;116:51–8.
[7] Scharnowski S, Kähler CJ. Particle image velocimetry-Classical operating rules from today's perspective. Opt Lasers Eng 2020;135:106185.
[8] Choi YS, Seo KW, Sohn MH, Lee SJ. Advances in digital holographic micro-PTV for analyzing microscale flows. Opt Lasers Eng 2012;50:39–45.
[9] Meier W, Boxx I, Arndt C, Gamba M, Clemens N. Investigation of auto-ignition of a pulsed methane jet in vitiated air using high-speed imaging techniques. J Eng Gas Turbine Power 2011;133.
[10] Altamura D, Lassandro R, Vittoria F, De Caro L, Siliqi D, Ladisa M, Giannini C. X-ray microimaging laboratory (XMI-LAB). J Appl Crystallogr 2012;45:869–73.
[11] Lee SJ, Huh JK, Kim GB. Measurements of Flow inside Microchannels Using Micro-PIV and X-ray Micro-imaging Techniques. In: Proceedings of the APS division of fluid dynamics meeting abstracts; 2001. pp. JQ. 006.
[12] Bohl DG, Koochesfahani MM. Molecular tagging velocimetry measurements of axial flow in a concentrated vortex core. Phys Fluids 2004;16:4185–91.
[13] Kobatake M, Takaki T, Ishii I. A real-time micro-PIV system using frame-straddling high-speed vision. In: Proceedings of the IEEE international conference on robotics and automation. IEEE; 2012. p. 397–402.
[14] Hart DP. Super-resolution PIV by recursive local-correlation. J Vis 2000;3:187–94.
[15] Sugii Y, Nishio S, Okuno T, Okamoto K. A highly accurate iterative PIV technique using a gradient method. Meas Sci Technol 2000;11:1666.
[16] Zhang ZB, Ye JQ, Deng QW, Zhong JG. Image-free real-time detection and tracking of fast moving object using a single-pixel detector. Opt Express 2019;27:35394–401.
[17] Zhang Z, Wang X, Zheng G, Zhong J. Fast Fourier single-pixel imaging via binary illumination. Sci Rep 2017;7:1–9.
[18] Shi D, Yin K, Huang J, Yuan K, Zhu W, Xie C, Liu D, Wang Y. Fast tracking of moving objects using single-pixel imaging. Opt Commun 2019;440:155–62.
[19] Qiu Z, Zhang Z, Zhong J. Comprehensive comparison of single-pixel imaging methods. Opt Lasers Eng 2020;134:106301.
[20] Gao X, Deng H, Ma M, Guan Q, Sun Q, Si W, Zhong X. Removing light interference to improve character recognition rate by using single-pixel imaging. Opt Lasers Eng 2021;140:106517.
[21] Ma M, Zhang Y, Deng H, Gao X, Gu L, Sun Q, Su Y, Zhong X. Super-resolution and super-robust single-pixel superposition compound eye. Opt Lasers Eng 2021;146:106699.
[22] Deng H, Wang G, Li Q, Sun Q, Ma M, Zhong X. Transmissive Single-Pixel Microscopic Imaging through Scattering Media. Sensors 2021;21:2721.
[23] Brenner C, Boehm J, Guehring J. Photogrammetric calibration and accuracy evaluation of a cross-pattern stripe projector, Videometrics VI. Inter Soc Opt Photon 1998:164–72.
[24] Hazel AL, Heil M. The steady propagation of a semi-infinite bubble into a tube of elliptical or rectangular cross-section. J Fluid Mech 2002;470:91–114.
[25] Olanrewaju A, Beaugrand M, Yafia M, Juncker D. Capillary microfluidics in microchannels: from microfluidic networks to capillaric circuits. Lab Chip 2018;18:2323–47.
[26] Konda PC, Loetgering L, Zhou KC, Xu S, Harvey AR, Horstmeyer R. Fourier ptychography: current applications and future promises. Opt Express 2020;28:9603–30.
[27] Deng H, Gao X, Ma M, Yao P, Guan Q, Zhong X, Zhang J. Fourier single-pixel imaging using fewer illumination patterns. Appl Phys Lett 2019;114:221906.